Correlation transitions in the Ising chain with competing short-range and long-range mirror interactions

István Daruka[1] and Zsolt Gulácsi[2]
[1]Department of Physics, University of Notre Dame, Notre Dame, Indiana 46556
[2]Department of Theoretical Physics, Lajos Kossuth University, H-4010 Debrecen, Hungary

(Received 30 April 1998)

We present exact four-spin- and string-correlation functions derived for an Ising chain with competing geometrical nearest-neighbor short-range and mirror-image-type long-range interactions. Unusual $T\neq 0$ correlation effects were found, indicating qualitative changes in the behavior of the system in different T domains. These domains are not separated by a sharp, traditional phase transition, but are delimited by a temperature T_i at which the exact connected four-spin-correlation function vanishes. At the same T_i the pair-correlation function changes its character: The functional form of the correlation length and the nature of the long-range decay are modified. [S1063-651X(98)09610-X]

PACS number(s): 64.60.Cn, 02.70.Lq, 05.50.+q

I. INTRODUCTION

The competition between long- and short-range interactions in low-dimensional spin systems has been extensively studied recently. The unusual properties caused by competing interactions, the common sources of frustration, make these spin systems relevant to the description of a wide variety of physical phenomena. Applications span over the following fields and effects. The crossover between the half integer and integer spin-chain behavior implemented by spin ladders with competing interactions enables us to study the effects emerging in connection with the Haldane conjecture [1]. Several material properties can be modeled using coupled chains for heavy fermions, Kondo lattices, and spin-Peierls systems [2]. One can analyze the dimensional crossovers in magnetic systems, in particular from chains to square lattices [3]. The first-order quantum phase transitions in one dimension [4] can be studied with the help of one-dimensional spin systems. Coupled spin-chain models allow us to investigate the development of D-dimensional magnetic long-range order at $T=0$ associated with interchain coupling [5]. Low-dimensional spin systems can also be used to get insight into the nature of unusual ordering effects including local, topological, or hidden ordering [6] that also relate to surface physics [7]. High-T_c superconductivity or the Tomonaga-Luttinger liquids can be approached via Sr-Cu-O ladders [8].

These applications cover a large spectrum of models, including classical, Ising, and quantum systems. The interplay between the different systems may be used to get insight into the nature of short-range ordering and finite-range ordering in quantum systems [2] or even to relate the $T=0$ quantum aspects to the $T\neq 0$ classical behavior [9].

Low-dimensional Ising spin systems are important in this field since they serve as an intermediate step between the classical and quantum limits. In spite of their striking simplicity [10], Ising systems are complex, exhibiting an extremely interesting behavior [11]. As examples, low-dimensional Ising models containing competing interactions have been used to give a coarse-grained representation of frustrated phase separation in high-T_c superconductors [12], to analyze the phase stability of metallic alloys [13], to analyze surface properties [14], to describe immunological reactions in biological systems [15], and to describe fractal properties and chaotic behavior [16] or even real compounds such as TMCON [17].

From the great variety of long-range interactions used in these models, we concentrate on the mirror-image type-interactions [20]. Their importance has been emphasized by Sahimi and Stauffer [15], who proposed an Ising model with mirror-image-type interactions in order to describe idiotypic–anti-idiotypic immunological networks in connection with natural immune systems. Simons and Altshuler [21] studied a spin-1/2 Heisenberg antiferromagnetic spin chain based on an exchange between the spins and their images via an inverse square pairwise potential. They showed that this system reveals a multiplet structure similar to Haldane-Shastry model [22]. Furthermore, de Boer *et al.* [23] pointed out that the structured patterns that emerge in such systems are reminiscent of those occurring in spinodal decomposition. We note that the latter process is of great interest due to its relevance in different decomposition scenarios in order-disorder system transformations or in self-organization [23].

The above considerations motivate us to find and study the exact solution of an Ising chain with competing interactions. In particular, we consider mirror-image-type long-range interactions together with short-range components consisting of geometrical nearest-neighbor couplings. The system is equivalent to two coupled Ising chains with short-range interactions only, which are obtained by folding the system about its geometrical center position. Besides the properties related to strange local ordering effects at $T\neq 0$ (screening effects in correlation functions or local ordering that can only be detected far-away from the position where it emerges), the paper presents an exact calculation of four-spin- and string-correlation functions for a nontrivial case [24]. Using these concepts, a completely new, phase-transition-like behavior was found. We find qualitative differences in the behavior of the system in different tempera-

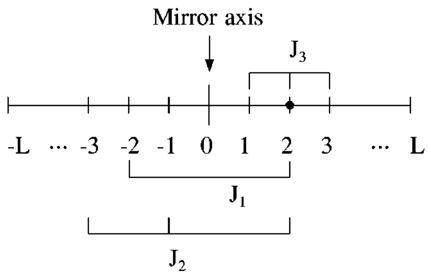

FIG. 1. Illustration of the model. Each of the $2N$ spins interacts with its mirror image, with the two neighbors of its mirror image and with the two geometrical neighbors. The coupling strengths are J_1, J_2, and J_3, respectively.

ture domains that are not separated by a sharp, traditional phase transition, but are delimited by a temperature T_i at which the exact connected four-spin-correlation function vanishes. At the same T_i the pair-correlation function changes its character: The functional form of the correlation length and the nature of the long-range decay are modified. We interpreted this behavior as a peculiar frustration effect of the competing interactions.

We mention that similar effects called correlation transitions emerging at the ''disorder line'' in the phase diagram have been found in other Ising systems as well [18]. The disorder line corresponds to a local minimum in the correlation length in the form of a cusp [18]. As will be shown below, in our case this is not necessarily true. The T_i temperature deduced by us in the present model is related to zeros of the four-spin correlation function.

The paper is structurated as follows. In Sec. II we present the model together with the deduced results. A summary in Sec. III closes the presentation.

II. MODEL AND OBTAINED RESULTS

We consider an open chain of $N=2L$ localized $S_{i,\alpha}=\pm 1$ spins with a mirror-image center O at its geometrical center position. Here $i=1,\ldots,L$ indicates the distance d_i from O and $\alpha=1,2$ denotes the right (left) [1 (2)] side of the chain with respect to O (Fig. 1). With these notations and $H_N=\tilde{H}_N-(J_1+J_3)S_{1,1}S_{1,2}$, our Hamiltonian H_N is given by

$$\tilde{H}_N=-\sum_{i=1}^{L-1}\Bigg[J_1S_{i+1,1}S_{i+1,2}+J_2(S_{i,1}S_{i+1,2}+S_{i,2}S_{i+1,1})+\sum_{\alpha=1,2}J_3(S_{i,\alpha}S_{i+1,\alpha})\Bigg], \tag{1}$$

with the long range mirror-image interaction J_1, the interaction with the nearest neighbors of the mirror image J_2, and short-range couplings with the geometrical nearest neighbors J_3. For example, in natural immune system models, a so-called T cell collects information about the invading virus via the J_1 and J_2 interactions, while the coupling J_3 invokes an information restoring mechanism: The T cell tries to reproduce some missing information about the virus simply by interpolation. To emphasize the connection with ladder problems, note that H_N also describes two coupled chains [19], which are obtained by folding the system about the point O. In the following, we make use of the procedure presented in Ref. [20] and extend it to handle the mirror-image and geometrical neighbor interactions simultaneously to give an exact solution for the model.

The partition function is obtained by summing up the spin-pair contributions $(S_{k,1};S_{k,2})$, in steps for a fixed k, starting from $k=L$, and decreasing k by unity at each further step. A recurrence relation emerges and the penultimate step gives

$$\frac{Z_N}{2^{L-1}}=\sum_{S_{1,1},S_{1,2}}e^{\beta(J_1+J_3)S_{1,1}S_{1,2}}\Bigg[\sum_{p=\pm 1}K_{L-1}^{p}V(p,S_{1,1},S_{1,2})\Bigg],$$

$$\begin{pmatrix}K_{l+1}^{(1)}\\ K_{l+1}^{(-1)}\end{pmatrix}=M_0\cdot\begin{pmatrix}K_{l}^{(1)}\\ K_{l}^{(-1)}\end{pmatrix},$$

where the coefficients $K_l^{(p)}$ are determined recursively for $1\leqslant l\leqslant L-1$ and $K_1^{(p)}=1$. We have $\beta=1/k_BT$, $V(p,x,y)=\exp(p\beta J_1)\cosh[\beta(J_2+pJ_3)(x+py)]$, and M_0 is a 2×2 matrix given by $(M_0)_{n,m}=\delta_{n,m}\phi[(-1)^{n+1}]+(1-\delta_{n,m})\exp[(-1)^{n+1}\beta J_1]$, $\phi[x]=V(x,2,0)$, with eigenvalues

$$\lambda_i=(0.5)\{\phi[+1]+\phi[-1]+(-1)^{i+1}[4+(\phi[+1]-\phi[-1])^2]^{1/2}\},\quad i=1,2. \tag{2}$$

Introducing the 1×2 row vector $\hat{a}_2=(a_{2,1},a_{2,2}), a_{2,i}=\exp[-(-1)^i\beta(J_1+J_3)]$, and the 2×1 column vector $\hat{a}_1$ with elements $a_{i,1}=1$, the partition function

$$Z_N=2^L\{K_L^{(1)}\hat{a}_{2,1}+K_L^{(-1)}\hat{a}_{2,2}\} \tag{3}$$

can be written as $Z_N=2^L\hat{a}_2M_0^{L-1}\hat{a}_1$. Using $x_i=-[1/\{(\phi[+1]-\lambda_i)c\}], c=\exp(\beta J_1)$, and $W_i=[x_i\hat{a}_{2,1}+\hat{a}_{2,2}]/(x_1-x_2)^2$ $(i=1,2)$, we obtain

$$Z_N=2^L(x_1-x_2)\sum_{i=1,2}(-1)^i(x_{3-i}-1)W_i\lambda_i^{L-1}. \tag{4}$$

In the thermodynamic limit, Z_N is determined by the highest eigenvalue. Since $\lambda_1>\lambda_2$ the free energy per spin becomes $f=-(k_BT/2)\ln(2\lambda_1)$. The specific heat can also be expressed as $C/k_B=-T[\partial^2f/\partial T^2]=(t/2)[\partial^2\{t\ln(2\lambda_1)\}/\partial t^2]$, where $t=k_BT/J_1$. Except for the $T\rightarrow 0$ limit, divergences in C are not present and a Shottky-type maximum emerges in the specific heat at $T_m\approx(1/k_B)\max_{i=1,2,3}\{J_i\}$ (Fig. 2).

For the pair correlation function we applied the same procedure as used for Z_N. We have

$$Z_N\Gamma_N^2((p,\alpha);(q,\beta))=\mathrm{Tr}[S_{p,\alpha}S_{q,\beta}\exp(-\beta H_N)]$$

$$=\sum_{\{S_{1,1},\ldots,S_{L,2}\}}S_{p,\alpha}S_{q,\beta}\exp(-\beta H_N),$$

where without a loss of generality, we choose $1\leqslant p\leqslant q\leqslant L$. The final result is

$$Z_N\Gamma_N^2((p,\alpha);(q,\beta))=2^L\hat{a}_2M_0^{p-1}\sigma_3^{|\alpha-\beta|}M_1^{q-p}M_0^{L-q}\hat{a}_1, \tag{5}$$

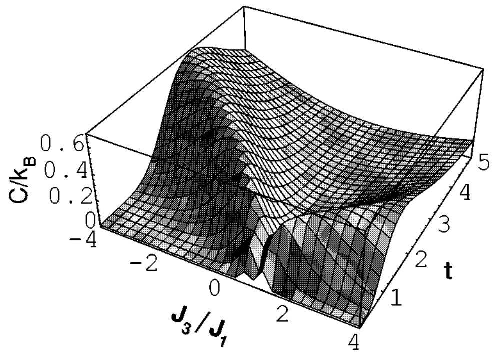

FIG. 2. Specific heat (C/k_B) as a function of the scaled temperature ($t=k_BT/J_1$) and the scaled coupling strength J_3/J_1. We used $J_2/J_1=1$ for this plot.

where $(M_1)_{i,i}=\gamma_i=\exp[(3-2i)\beta J_1]\sinh[2\beta\{J_3+(3-2i)J_2\}]$ is a diagonal matrix. Using the eigenvalues of M_0 one can write

$$Z_N\Gamma_N^2((p,\alpha);(q,\beta))=2^L\sum_{i,j,k=1,2}(-1)^{i+j+k+1}\delta^{j-1}\times(1-x_{3-k})x_lW_i\lambda_i^{n_1}\gamma_j^{n_2}\lambda_k^{n_3}, \quad (6)$$

where $l=(3-i)(j-1)+(2-j)k, \delta=(-1)^{|\alpha-\beta|}, n_1=p-1, n_2=q-p$, and $n_3=L-q$. In the thermodynamic limit the pair-correlation function takes the form

$$\Gamma^2=\lim_{N\to\infty}\Gamma_N^2=[x_1\rho_1^{n_2}-\delta x_2\rho_2^{n_2}-rx_1\rho_3^{n_1}(\rho_1^{n_2}-\delta\rho_2^{n_2})]/[x_1-x_2], \quad (7)$$

where $\rho_1=\gamma_1/\lambda_1, \rho_2=\gamma_2/\lambda_1, \rho_3=\lambda_2/\lambda_1$, and $r=W_2/W_1$. As can be seen, three types of correlation lengths emerge, $\xi_i=-1/\ln\rho_i$, $i=1,2,3$. Obviously ξ_3 characterizes the effect of the inhomogeneity induced by the mirror center.

The four types of correlation behavior are illustrated in Fig. 3. One ferromagnetic [Fig. 3(a)] and three types of antiferromagnetic decay were obtained. Each of these decays correspond to a long-range order at $T=0$ (see Fig. 6) of which (a) and (b) are symmetric and (c) and (d) are antisymmetric to the mirror center.

Making use of Eq. (6), we also derived an expression for the magnetic susceptibility that reduces to

$$\chi=\frac{(g\mu_B)^2}{J_1}[2x_1(1+\rho_1)]/[t(x_1-x_2)(1-\rho_1)] \quad (8)$$

in the thermodynamic limit. Divergences in χ are not present except in the ferromagnetic case (domain I in Fig. 6) in the $T\to 0$ limit [Fig. 4(a)]. Characteristic behaviors for χ are contained in Fig. 4.

The four-spin-correlation function

$$Z_N\Gamma_N^4=\sum_{\{S_{1,1},\ldots,S_{L,2}\}}S_{p,\alpha}S_{q,\beta}S_{r,\mu}S_{s,\nu}\exp(-\beta H_N)$$

for $1\leqslant p\leqslant q\leqslant r\leqslant s\leqslant L$ was deduced via the same transfer matrix method. We find

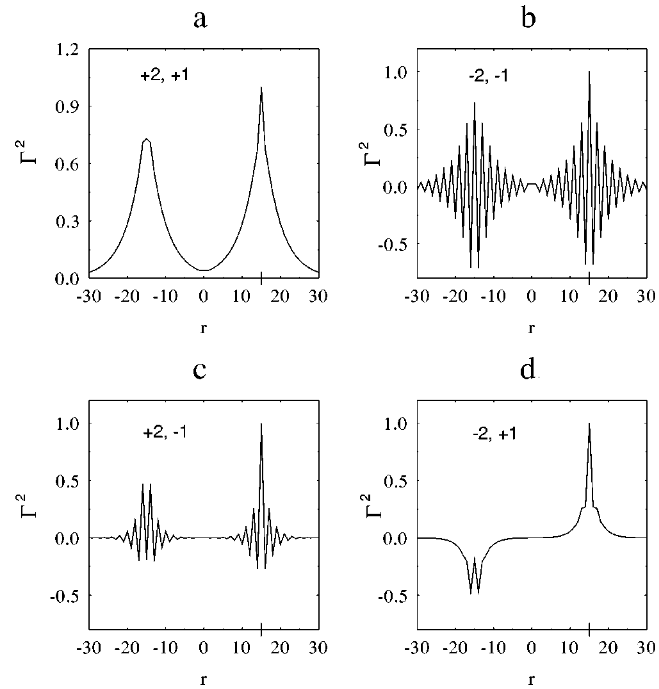

FIG. 3. Pair-correlation function as a function of the spin positions. One of the spins was fixed at the chain position $r=15$, while the other one was moved along the linear chain. The scaled temperature ($t=k_BT/J_1$) used for this plot was $t=4$. Four types of behavior were obtained by varying the coupling constants J_2/J_1 and J_3/J_1, whose values can be read from the plot. One ferromagnetic and three antiferromagnetic types of decay can be seen. The decays (a) and (b) are symmetric, while (c) and (d) are antisymmetric with respect to the mirror center. The corresponding coupling constant domains can be seen in Fig. 6.

$$Z_N\Gamma_N^4=2^L\hat{a}_2M_0^{p-1}\sigma_3^{|\alpha-\beta|}M_1^{q-p}M_0^{r-q}\sigma_3^{|\mu-\nu|}M_1^{s-r}M_0^{L-s}\hat{a}_1, \quad (9)$$

and using $k_1=(3-i)(j-1)+(2-j)k, k_2=(l-1)(3-m)+(2-l)i$, $\delta=(-1)^{|\alpha-\beta|}$, $\varepsilon=(-1)^{|\mu-\nu|}$, $m_1=r-q$, $m_2=s-r, m_3=L-s, m_4=q-p$, and $m_5=p-1$ we obtain

$$\frac{\Gamma_N^4}{2^L}=\sum_{i,j,k,l,m=1,2}\frac{(-1)^{i+j+k+l+m+1}}{Z_N}\times\varepsilon^{j-1}\delta^{l-1}\frac{(1-x_{3-k})x_{k_1}x_{k_2}}{(x_1-x_2)}W_m\lambda_i^{m_1}\gamma_j^{m_2}\lambda_k^{m_3}\gamma_l^{m_4}\lambda_m^{m_5}. \quad (10)$$

In the thermodynamic limit the summation gives

$$\begin{aligned}\Gamma^4=&\lim_{N\to\infty}\Gamma_N^4\\=&\{r\rho_3^{m_5}[\rho_3^{m_1}A(m_2,m_2,x_1,x_1;\varepsilon)A(m_4,m_4,x_2,x_1;\delta)\\&-A(m_2,m_2,x_1,x_2;\varepsilon)A(m_4,m_4,x_1,x_1;\delta)]\\&+A(m_2,m_2,x_1,x_2;\varepsilon)A(m_4,m_4,x_1,x_2;\delta)\\&-\rho_3^{m_1}A(m_2,m_2,x_1,x_1;\varepsilon)A(m_4,m_4,x_2,x_2;\delta)\}\theta_1,\end{aligned} \quad (11)$$

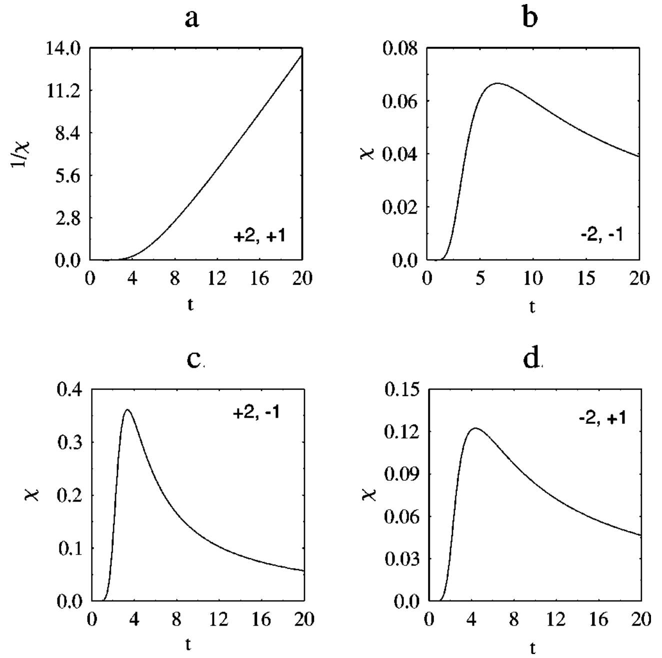

FIG. 4. Magnetic susceptibility [in units of $(g\mu_B)^2/J_1$] as a function of the scaled temperature ($t=k_BT/J_1$). Two types of behavior were obtained for different values of couplings. For a certain range of couplings (domain I in Fig. 6) we get a ferromagnetic divergence at $t=0$ (a). The values of the scaled coupling constants J_2/J_1 and J_3/J_1 can be read from the plot.

where $A(i,j,x,y;a)=x\rho_1^i-ay\rho_2^j$ and $\theta_m=W_m/W_1(x_1-x_2)^2$. It can be seen that Γ^4 consists of two parts. The first one, containing the factor $\rho_3^{m_5}$, characterizes the influence of the inhomogeneity induced by the mirror center. The second part (independent of ρ_3) can be considered as the ''homogeneous'' contribution. The decay of Γ^4 is determined by ρ_3 if $r-q\rightarrow\infty$ and by $\max\{|\rho_1|,|\rho_2|\}$ if $s-r\rightarrow\infty$ or $q-p\rightarrow\infty$. The connected part of Γ^4 given by $\Gamma_c^4(1,2,3,4)=\Gamma^4(1,2,3,4)-\Gamma^2(1,2)\Gamma^2(3,4)$ becomes

$$\Gamma_c^4=\frac{\rho_3^{m_1}A(m_2,m_2,1,1;\varepsilon)}{(x_1-x_2)^2}[rx_1\rho_3^{m_5}\{A(m_4,m_4,x_2,x_1;\delta)+\rho_3^{m_4}A(m_4,m_4,x_1,x_2;\delta)\}-A(m_4,m_4,1,1;\delta)A(0,0,x_1x_2,r^2x_1^2;\rho_3^{m_4+2m_5})]. \tag{12}$$

Increasing the distance m_1 between the pairs, the decay of Γ_c^4 is governed by ρ_3. The four typical behaviors are illustrated in Fig. 5.

Being interested also in the study of local ordering, we derived an exact string-correlation expression. We start with the definition

$$Z_N\mathcal{L}_n=\mathrm{Tr}S_1S_2\cdots S_n\exp(-\beta H_N)=\sum_{S_i=\pm1}S_1S_2\cdots S_n\exp(-\beta H_N),$$

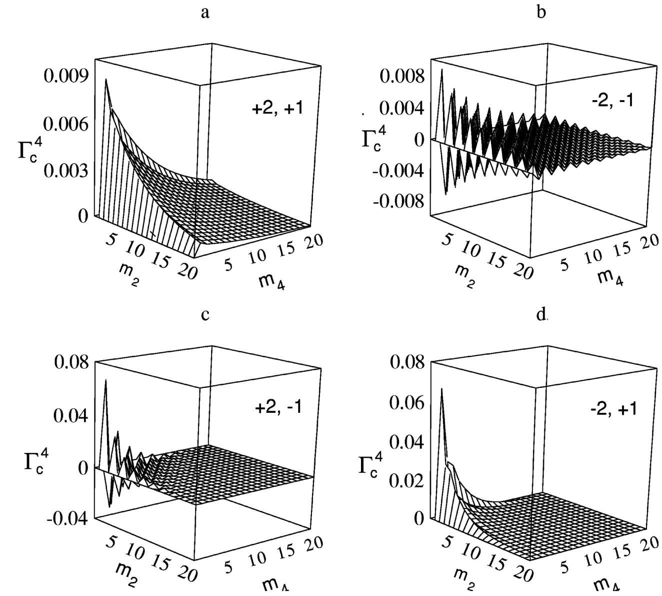

FIG. 5. Four-point correlation function as a function of the spin separations m_2 and m_4 (see the text) for different sets of coupling constants J_2/J_1 and J_3/J_1 displayed in the figure. The corresponding scaled temperature is $t=10/3$. Both smooth and oscillatory decays can be seen.

where $S_1,S_2,\ldots,S_n$ denotes a particular sequence of n adjacent spins. Then, using the same strategy as for the four-spin correlation function, the following explicit formula can be obtained [$\tilde{\mathcal{L}}_n=(x_1-x_2)(d_1-d_2)\mathcal{L}_n,\varrho(n)=\rho_5^{n/2}-\rho_6^{n/2}$]:

$$\tilde{\mathcal{L}}_n=\sum_{p=\pm1}y_p\{x_1[x_p\varrho(n)-(d_1\rho_5^{n/2}-d_2\rho_6^{n/2})]+[d_1d_2\varrho(n)-x_p(d_2\rho_5^{n/2}-d_1\rho_6^{n/2})]\}, \tag{13}$$

where i denotes the position of the first spin in the sequence, $y_1=\rho_3^{i-1}r,y_2=-1$, and $d_m=-b'/(a'-t_m),m=1,2$. The $a',b',t_1,t_2,\rho_5,\rho_6$ coefficients depend upon the arrangement

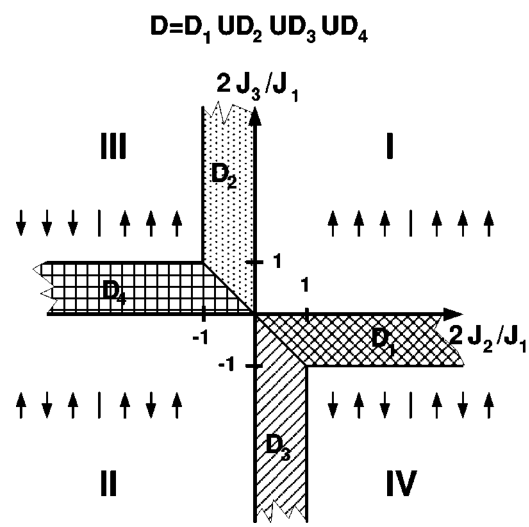

FIG. 6. $T=0$ phase diagram. The four types of long-range order appearing in the model are represented by six spins around the mirror center O (vertical line). The corresponding domains I, II, III, and IV are delimited by the solid lines.

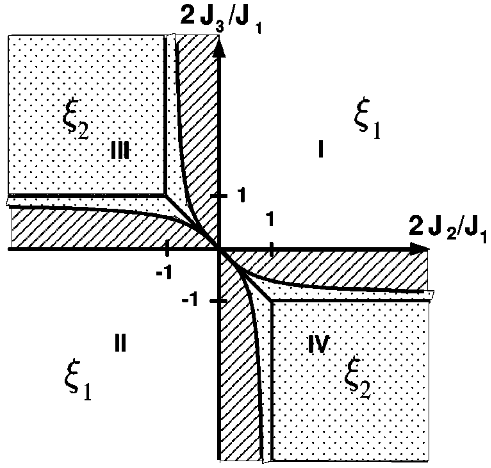

FIG. 7. $T\neq 0$ behavior of the model. In domain D (see Fig. 6), below the coupling dependent T_i, the dominant correlation length is ξ_1, which becomes ξ_2 for $T>T_i$. Thus, as we increase the temperature, the $T=0$, ξ_2 domains expand to the dotted area and at $T=\infty$ they reach the axes, occupying the hatched regions as well.

of the spins considered [26]. We emphasize that $\mathcal{L}_n$ always vanishes at $T\neq 0$ in the $n\to\infty$ limit. For the sake of consistency, we note that the $J_3\to 0$ limit is properly reobtained for all quantities presented above. In addition, the classical one-dimensional Ising results are recovered for $J_1=J_2=0$ or $J_1=J_3=0$ and the contraction of any spin pairs in Γ^4 leads to Γ^2.

In the $T=0$ phase diagram for $J_1>0$ (see Fig. 6) four different domains can be found: a ferro phase in region I

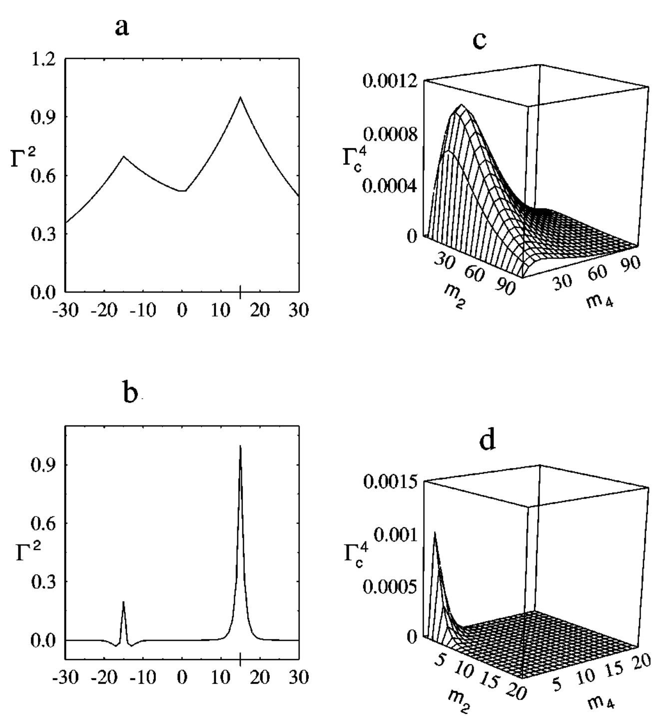

FIG. 8. Correlation behavior (for domain D_2 in Fig. 6) below ($t=0.474$) and above ($t=2.488$)T_i. We used $J_2/J_1=-0.4975$ and $J_3/J_1=0.995$ as scaled coupling constants for this plot. The pair-correlation function changes its character: The ferromagnetic decay below T_i becomes antiferromagnetic above T_i. The four-point correlation function behaves similarly, though it vanishes at T_i.

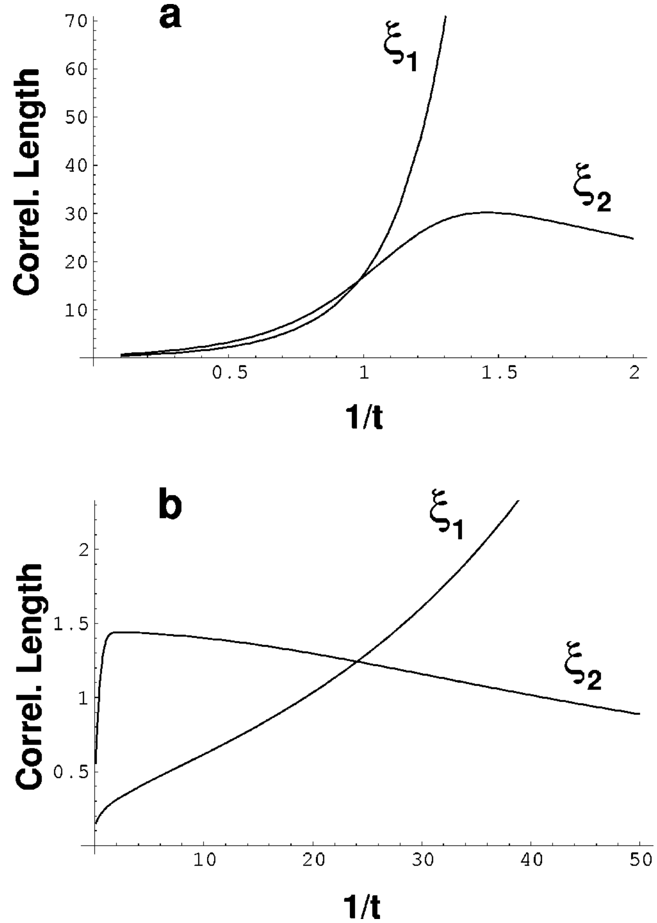

FIG. 9. Competing correlation lengths as a function of the scaled inverse temperature ($1/t$). At $1/T_i$ the two correlation lengths become equal, corresponding to a cusp in the dominating correlation length curve [$\max(\xi_1,\xi_2)$]. In (a) ($J_2/J_1=-0.4975$, $J_3/J_1=0.995$) the cusp does not appear as a local minimum, in contrast to (b) ($J_2/J_1=-0.4975$, $J_3/J_1=0.5025$), where the cusp is a local minimum of the dominating correlation length.

(which also contains the domains D_1 and D_2), an antiferro phase symmetric with respect to O in region II (which also contains the domains D_3 and D_4), striped antiferro order with ferro subchains in region III (observed also in competing Heisenberg spin ladders [25]), and striped antiferro order with antiferro subchains in region IV. At $T\neq 0$, in the presence of fluctuations, extremely interesting and unusual aspects emerge. The system does not exhibit a long-range order in this case, so one cannot speak about phase transitions in the usual context. However, the correlation functions in region D (see Fig. 6) behave qualitatively differently in different temperature regions, indicating that the system undergoes qualitative changes, even if these regions are not separated by a sharp, traditional phase transition. In region D, at $m_2>0$ and $\varepsilon=1$ (i.e., the third and fourth spins in Γ^4 are not identical and situated on the same side of the mirror center O) one can deduce a finite temperature T_i via the relation

$$\left|\frac{\sinh[2\beta_i(J_2+J_3)]}{\sinh[2\beta_i(J_2-J_3)]}\right|=\exp(-2\beta_i J_1), \qquad (14)$$

at which Γ_c^4 vanishes, independently of the spin positions. Although the four-point correlation function vanishes for any spins at T_i, it behaves qualitatively similar below [Fig. 8(c)] and above [Fig. 8(d)] T_i, illustrating the strangeness of this transition. Furthermore, at T_i the long-range behavior of the pair-correlation function Γ^2 changes its character. Thus, at T_i, the dominating correlation length in Γ^2, $\xi_1 = -1/\ln\rho_1 (T<T_i)$, becomes $\xi_2 = -1/\ln\rho_2$ $(T>T_i)$, making the long-range correlation behavior of the system strikingly different (Fig. 9). This transition is also illustrated in Fig. 7, where the leading correlation length domains are plotted for a finite temperature (dotted area). We also note that at T_i not only the functional form of the correlation length but also the nature of the long-range decay is changed. For example, in the subdomain D_2 the decay of Γ^2 is ferromagnetic for $T<T_i$ [Fig. 8(a)], independent of the side index (α) of its spin positions, while above T_i [Fig. 8(b)] we have $\Gamma^2>0$ for both spins on the same side of O, but an antiferromagnetic long-range decay is obtained for spins on the opposite side with respect to O, i.e., the type-I correlation behavior is replaced by type III (displayed in Fig. 6). Therefore, in the single-chain picture the strange local ordering effect, which stems from the competing interactions, can only be detected far away from the position where it emerges. Similarly, making use of the notations of Fig. 6, we witness in the domain D_1 a I$\rightarrow$IV type transition, in domain D_3 a II$\rightarrow$IV type transition, and in domain D_4 a II$\rightarrow$III type correlation behavior change. Also connected to changes in the pair-correlation function, for $2>\sum_{\alpha=\pm1} 2\alpha|(J_3+\alpha J_2)/J_1|$ and $0<J_3<J_2<J_1$ at $T\rightarrow 0$, Γ^2 is J_1 and mirror-image side independent and a smoothly decaying function of distance. This is in contrast to the high-T limit where Γ^2 becomes an oscillating function of the distance and side and J_1 dependent. Finally, in the domain $J_i>0$, $J_1,J_2 \ll 1, J_3 \gg 1$, at intermediate $\beta(J_1,J_2)$ temperatures, screening effects are present in the correlation functions, i.e., Γ^i's are insensitive to the spin-position modifications within finite chain portions, signaling again an unusual short-range-ordering effect.

We mention that correlation transitions were also found for the axial next-nearest-neighbor Ising (ANNNI) chain [18] at disorder lines in the phase diagram. In this case, the dominating correlation length $[\max(\xi_1,\xi_2)]$ exhibits a local minimum (in the form of a cusp), while in our model the emerging cusp is not necessarily a local minimum of the dominating correlation length (Fig. 9). Furthermore, in contrast to the ANNNI chain where one of the correlation lengths is always purely exponential, monotonic decay and the other one is oscillatory with a parameter-dependent wave number, in our model both of the competing correlations can be purely exponential, nonoscillatory decays (e.g., in the subdomain D_2 in Fig. 6) or if one of them is oscillatory (e.g., in the subdomain D_1 in Fig. 6), the wave number is constant, corresponding to an antiferromagnetic decay. Mentioning these differences, we have to emphasize that since the exact four-point correlation function is not known for the ANNNI chain, the connection between the disorder lines and the behavior of the four-point function cannot be clearly established at the moment.

III. SUMMARY

We presented a $T\neq 0$ exact solution for an Ising chain with competing geometrical nearest-neighbor short-range and mirror-image-type long-range interactions deducing exact four-spin- and string-correlation functions. With the help of these functions, unusual $T\neq 0$ correlation effects were found, indicating qualitative changes in the behavior of the system in different T domains that are not separated by a sharp, traditional phase transition. These domains are delimited by a temperature T_i at which the exact connected four-spin-correlation function vanishes. The described phase-transition-like process is provided by a frustration effect of competing interactions. We expect similar behavior to occur in other systems where competing interactions are present as well.

ACKNOWLEDGMENTS

The research of Zs.G. was supported by OTKA-022874 and AKP-96/2-626/2.2 contracts. I.D. is grateful to the Kereskedelmi Bank Rt. Univ. Foundation for financial support.

[1] S. R. White, Phys. Rev. B **53**, 52 (1996); F. D. M. Haldane, Phys. Lett. **93A**, 464 (1983).
[2] S. P. Strong and A. J. Millis, Phys. Rev. Lett. **69**, 2419 (1992); I. Affleck (unpublished); J. Zang, A. R. Bishop, and D. Schmeltzer, Phys. Rev. B **52**, 6723 (1995).
[3] S. Chakraverty, Phys. Rev. Lett. **77**, 4446 (1996); E. Dagotto and T. M. Rice, Science **271**, 618 (1996).
[4] A. Kolezhuk, R. Roth, and U. Schollwöck, Phys. Rev. Lett. **77**, 5142 (1996).
[5] Z. Wang, Phys. Rev. Lett. **78**, 126 (1997).
[6] R. Chitra, S. Pati, H. R. Krishnamurthy, D. Sen, and S. Ramasesha, Phys. Rev. B **52**, 6581 (1995).
[7] K. Hida, Phys. Rev. B **45**, 2207 (1992); P. J. M. Bastiaansen and H. J. F. Knops, *ibid.* **53**, 126 (1996).
[8] M. Azuma (unpublished).
[9] U. Schollwöck, T. Jolicoeur, and T. Garel, Phys. Rev. B **53**, 3304 (1996).
[10] Y. Muraoka, K. Oda, J. W. Tucker, and T. Idogaki, J. Phys. A **29**, 949 (1996).
[11] M. Kardar and M. Kaufman, Phys. Rev. Lett. **51**, 1210 (1983); P. Bak and R. Bruinsma, *ibid.* **49**, 249 (1982).
[12] U. Löw, V. J. Emery, K. Fabritius, and S. A. Kivelson, Phys. Rev. Lett. **72**, 1918 (1994).
[13] M. Sobkowicz and B. Chakraborty, J. Stat. Phys. **83**, 739 (1996).
[14] P. J. M. Bastiansen and H. J. F. Knops, Phys. Rev. B **53**, 126 (1996).
[15] M. Sahimi and D. Stauffer, Phys. Rev. Lett. **71**, 4271 (1993).
[16] W. Jezewski, J. Stat. Phys. **82**, 1099 (1996).
[17] M. Mito *et al.*, J. Phys. Soc. Jpn. **64**, 4402 (1995).
[18] W. Selke, Phys. Rep. **170**, 213 (1988).
[19] In this case, i is the ladder step position, while α is the chain index within the ladder.

[20] M. Hunyadi and Zs. Gulácsi, Phys. Rev. B **53**, 2326 (1996).
[21] B. D. Simons and B. L. Altshuler, Phys. Rev. B **50**, 1102 (1994).
[22] F. D. M. Haldane, Phys. Rev. Lett. **60**, 635 (1988); B. S. Shastry, *ibid.* **60**, 639 (1988).
[23] R. J. de Boer *et al.*, in *Thinking about Biology*, edited by F. J. Varela and W. D. Stein (Addison-Wesley, New York, 1992).
[24] That is when Γ^4 or $\mathcal{L}_n$ cannot be expressed as a product of Γ^2 terms.
[25] A. K. Kolezhuk and H. J. Mikeska, Phys. Rev. B **53**, R8848 (1996).
[26] For all $S_{i,\alpha}$ with the same α, $a'=\psi(+1)$, $b'=\tau\psi(-1)$, $\psi(x)=[0.5\exp(2xJ_1\beta)]\sinh[4(J_3+xJ_2)\beta]$, $\rho_{5/6}=t_{1/2}/\lambda_1^2$, $\tau=+1$, $t_{1/2}=0.5((a'+b')+(+/-)\{(a'-b')^2+4\tau\sinh[2(J_2+J_3)\times\beta]\sinh[2(J_3-J_2)\beta]\}^{1/2})$. Alternating sequence of subsequent spin positions on different sides of O gives the same results as before with $\tau=-1$. For a symmetric adjacent spin sequence (O in the middle) $a'=\phi[1]=a, b'=\exp(-J_1\beta), b=\phi[-1]$, $t_{1/2}=0.5\{(a-b)+(+/-)[(a+b)^2-4]^{1/2}\}$, and $\rho_{5/6}=t_{1/2}/\lambda_1$.